Effect of Electromagnetic Interference on Integrated Circuits

Andreas Czylwik, University of Duisburg-Essen, Germany
Stefan Bieder, University of Duisburg-Essen, Germany
Sebastian Tonder, University of Duisburg-Essen, Germany
Sven Fisahn, Bundeswehr Research Institute for Protective Technologies and CBRN Protection, Germany
Martin Schaarschmidt, Bundeswehr Research Institute for Protective Technologies and CBRN Protection, Germany

1 Introduction

Critical infrastructure may be disturbed by high power electromagnetic (HPEM) weapons. Both, short impulses and modulated/unmodulated radio frequency (RF) carrier signals may be used. The interfering electromagnetic waves may be coupled by lines between different electronic devices to the inputs or outputs of integrated circuits (ICs) [1]. By shielding the lines or the use of twisted symmetric transmission lines, this effect may be significantly reduced. On the other hand, ICs themselves are influenced by HPEM pulses. A quantitative estimate of the coupling of HPEM waves to lines on an IC itself is required to investigate the effectiveness of applicable protective measures against them.

2 HPEM Wave Coupling on ICs without Protection Measures

The interference voltages resulting from coupling of HPEM waves to ICs without protective measures are investigated using EM field simulations.

2.1 Simulation Setup

A highly simplified model for transmission lines in an IC is analyzed using the 3D finite-difference time domain (FDTD) EM simulation software, Empire XPU™ [3]. The investigated IC model is shown in Figure 1.

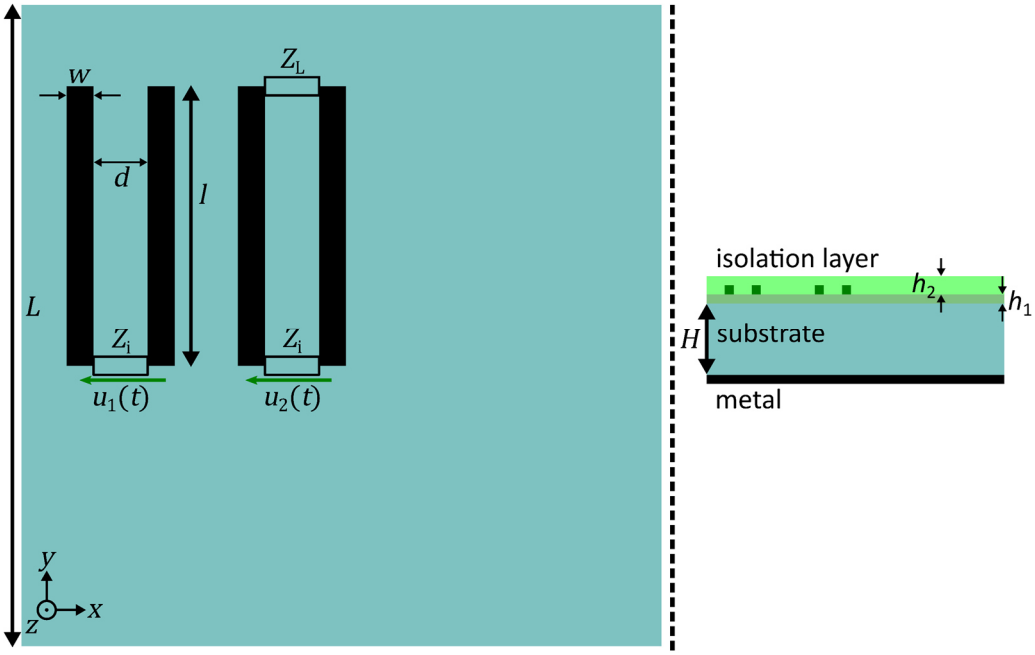

Figure 1: IC model, top view (left) and cross section (right)

Two test structures are used to obtain the interference voltages $u_1(t)$ and $u_2(t)$, respectively which are caused by the HPEM wave. The test structures are two parallel pairs of conductors of length l, each connected to a measurement port with input impedance Z_i, where the interference voltage is measured. The conductors of the test structure 1 (TS1), shown on the left, are not connected at the end of the pair of conductors which results in an open circuit. The conductors of the test structure 2 (TS2), shown on the right, are connected to the load impedance Z_L. The test structures are located on a cuboid of silicon with relative permittivity $\epsilon_{\mathrm{r},1}$ and dissipation factor $\tan(\delta_1)$. The cuboid has a square base with an edge length L and a height H. At the bottom of the cuboid there is a continuous metallic contact surface. The conductors are embedded in an isolation layer with relative permittivity $\epsilon_{\mathrm{r},2}$. The height h_1 indicates the distance between the silicon substrate and the test conductors, and the height h_2 indicates the thickness of the remaining isolation layer. Table 1 lists the values for all parameters of the IC model and the test structures.

Edge length	$L = 1\,\mathrm{mm}$
Substrate height	$H = 200\,\mu\mathrm{m}$
Input impedance	$Z_\mathrm{i} = 200\,\mathrm{k\Omega} + \frac{1}{\mathrm{j}\omega\ 200\,\mathrm{fF}}$
Load impedance	$Z_\mathrm{L} = 5\,\mathrm{k\Omega}$
Conductor length	$l = 300\,\mu\mathrm{m}$
Conductor spacing	$d = 20\,\mu\mathrm{m}$
Conductor width	$w = 10\,\mu\mathrm{m}$
Relative permittivity silicon	$\epsilon_{\mathrm{r},1} = 11.9$
Dissipation factor silicon	$\tan(\delta_1) = 0.01$
Relative permittivity isolation layer	$\epsilon_{\mathrm{r},2} = 3$
Isolation layer height, lower part	$h_1 = 8\,\mu\mathrm{m}$
Isolation layer height, upper part	$h_2 = 5\,\mu\mathrm{m}$

Table 1: Parameters of the IC model

Each test structure is modeled as a linear time-invariant system, and its field strength-to-voltage transfer function $H_n\,(\omega)$ is determined where $n \in \{1,2\}$ gives the number of the test structure. Here, the IC is exposed to the electric field of the HPEM wave $\mathbf{E}(t) = \left(\mathrm{E_x}(t), \mathrm{E_y}(t), \mathrm{E_z}(t)\right)^\mathrm{T}$. The magnitude of the exciting time-dependent field strength is denoted by $a(t) = |\mathbf{E}(t)|$ and the resulting interference voltage at the output of the test structures by $u_n\,(t)$. Since the relation between the magnitude of the field strength $a(t)$ and the voltage $u_n\,(t)$ is linear, with knowledge of the impulse response $h_n\,(t)$ and the corresponding transfer function $H_n\,(\omega) = \mathfrak{F}\{h_\mathrm{n}(t)\}$ the voltage can be calculated by $u_n(t) = \mathfrak{F}^{-1}\{H_n\,(\omega) \cdot A(\omega)\}$ for any input signal. Here, the operators $\mathfrak{F}$ and $\mathfrak{F}^{-1}$ denote Fourier transform and the inverse Fourier transform, respectively, and $A(\omega) = \mathfrak{F}\{a(t)\}$ is the Fourier transform of $a(t)$. The relationship between excitation and interference voltage is shown in Figure 2. It should be noted that for each combination of direction of incidence of the electromagnetic wave and wave polarization, a corresponding transfer function must be determined.

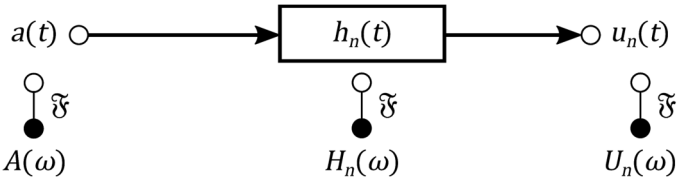

Figure 2: Schematic representation of the relationship between excitation and interference voltage

To determine the transfer functions, EM simulations are performed with a Gaussian excitation pulse [2]. The magnitude of the field strength of the Gaussian pulse has the shape

$$a(t)|_\mathrm{gauss} = E_0 \cdot \exp\left(-\left(\frac{t-t_0}{\tau}\right)^2\right), \tag{1}$$

with the maximum value of the field strength E_0. The bandwidth dependent time constant

$$\tau = \frac{\sqrt{\ln(10)}}{\pi B} \tag{2}$$

determines the duration of the Gaussian pulse, where B gives the 20-dB bandwidth of the pulse. The time shift $t_0 = \frac{\ln(10)\sqrt{5}}{\pi B}$ ensures that the Gaussian pulse is close to zero for negative times $t < 0$.

Using the Fourier transform for the interference voltage $U_n(\omega) = \mathfrak{F}\{u_n(t)\}$, resulting from the EM simulation, the transfer function $H_n(\omega) = U_n(\omega)/A(\omega)$ is calculated. The transfer functions of the test structures can be used to calculate interference voltages for any arbitrary shape of the exciting HPEM pulse. In particular, the interference voltages are also determined for a double-exponential excitation pulse [2]. The magnitude of the field strength of the double-exponential pulse (dexp) is

$$a(t)|_{\text{dexp}} = E_0 \cdot c \cdot (\exp(-\alpha \cdot t) - \exp(-\beta \cdot t)), \tag{3}$$

where the normalization factor is chosen such that $\max\{a(t)|_{\text{dexp}}\} = E_0$, hence:

$$c = [\max\{\exp(-\alpha \cdot t) - \exp(-\beta \cdot t)\}]^{-1} = \left[\left(\frac{\beta}{\alpha}\right)^{-\frac{\alpha}{\alpha-\beta}} - \left(\frac{\beta}{\alpha}\right)^{-\frac{\beta}{\alpha-\beta}}\right]^{-1}. \tag{4}$$

The parameters α and β determine the falling and the rising slope of the double-exponential pulse, respectively. The rise time t_{rise}, in which the pulse reaches 90% of its maximum value, is linked to the rise parameter by $\beta = \ln(9)/t_{\text{rise}}$. The full-duration-at-half-maximum time t_{fdhm}, which specifies the time duration between the first reaching and the second reaching of half of the maximum value, defines the falling parameter by $\alpha = \ln(2)/t_{\text{fdhm}}$.

The normalized magnitude of the frequency function of the excitation signal is given by normalizing the magnitude of frequency function to its maximum: $A_{\text{norm}}(\omega) = |A(\omega)|/\max\{|A(\omega)|\}$.

Figure 3 shows the shape of the excitation pulses as well as the corresponding normalized magnitude of the frequency functions. The maximum field strength is $E_0 = 50\ \text{kV/m}$. The rise time of the double-exponential pulse is $t_{\text{rise}} = 100\ \text{ps}$ and its full-duration-at-half-maximum time is $t_{\text{fdhm}} = 2\ \text{ns}$. The 20-dB bandwidth of the Gaussian pulse and the double-exponential pulse is $B|_{\text{gauss}} = 20\ \text{GHz}$ and $B|_{\text{dexp}} \approx 500\ \text{MHz}$, respectively.

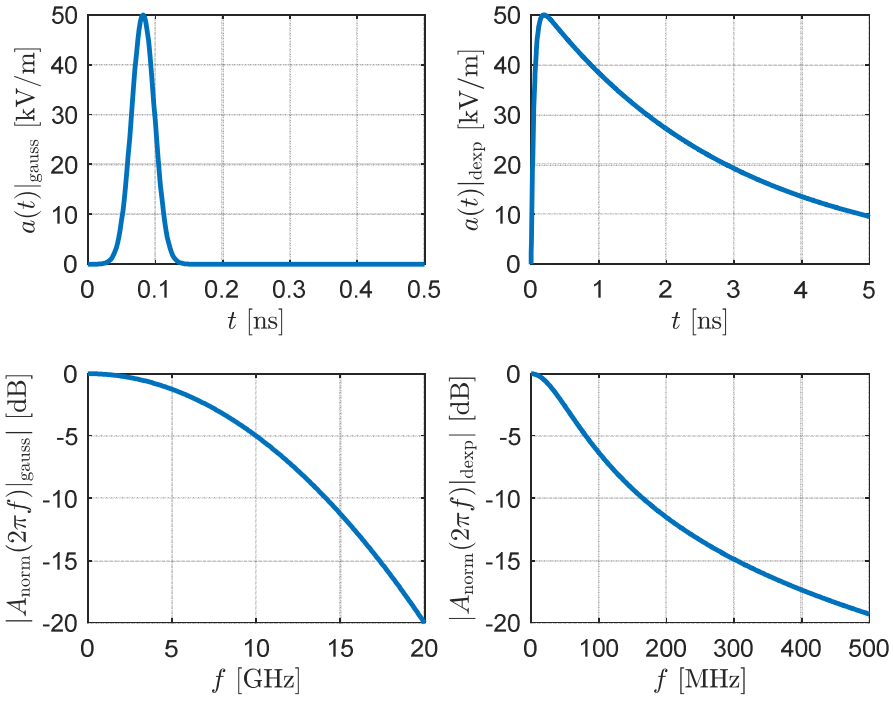

Figure 3: Gaussian excitation pulse (upper left) and double-exponential pulse (upper right) and corresponding normalized frequency functions (second row)

The two signals differ significantly in their shape. The Gaussian pulse has a short rising time, reaches its maximum after less than 100 ps and then falls again symmetrically to the rise, so that the signal has already decayed after less than 150 ps. The double-exponential pulse also has a short rising edge, but the falling edge is much longer. Although the drop to half of the maximum has already occurred after about 2 ns, after 5 ns the signal is still clearly different from zero.

2.2 Simulation Results

In the results presented here, different directions of incidence and polarizations of HPEM waves are considered. Since the electromagnetic wave is linearly polarized in all simulations, it can be uniquely described by specifying the wave propagation direction, i.e. the direction of the complex Poynting vector $\mathbf{S} = S \cdot \mathbf{e}_\mathrm{S}$ and the direction of the complex electric field vector $\mathbf{E} = E \cdot \mathbf{e}_\mathrm{E}$. Here S and $\mathbf{e}_\mathrm{S}$ give the complex magnitude and the unit vector of the Poynting vector, and E and $\mathbf{e}_\mathrm{E}$ give the complex magnitude and the unit vector of the electric field.
The interference voltage waveforms at the test ports are discussed for 3 different combinations of direction of incidence and polarization, where two combinations result in the highest peak interference voltage and one combination results in the lowest peak interference voltage. Referring to the coordinate system given in Figure 1, the direction of wave propagation and the polarization of the wave are chosen in x-, y- and z-direction, indicated by the unit vectors $\mathbf{e}_\mathrm{x}$, $\mathbf{e}_\mathrm{y}$ and $\mathbf{e}_\mathrm{z}$, respectively. Figure 4 and Figure 5 show the interference voltages at the test structures caused by excitation with a HPEM Gaussian pulse and double-exponential pulse, respectively. EM simulations have been carried out for a Gaussian excitation pulse, while the results for the double-exponential excitation pulse are calculated using the approach presented in the previous section.

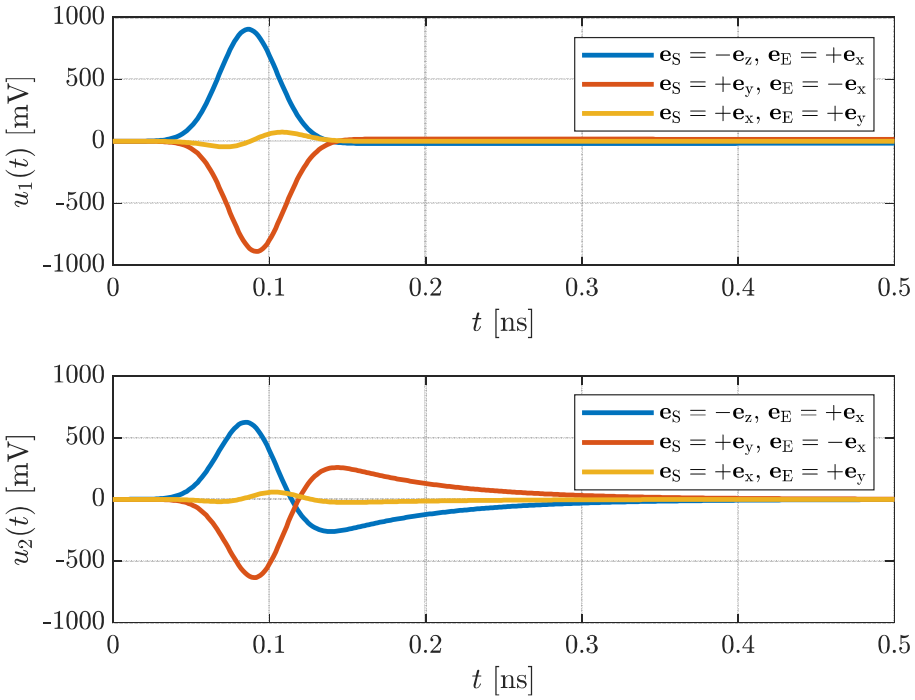

Figure 4: Interference voltages at the test structures without protection measures excited by a Gaussian pulse

For both excitation pulse shapes, the two cases with highest interference (HD) are caused by a HPEM wave propagating in the negative z-direction with its electric field oriented in the direction of the x-axis (blue lines) and a HPEM wave propagating in the y-direction with its electric field oriented in negative x-direction (red lines), respectively. Here, regardless of the shape of the excitation pulse, the magnitude of the interference voltage reaches a peak value of $\max\{|u_1(t)|\}|_\mathrm{HD} \approx 900\ \mathrm{mV}$ for the case of the open conductor pair (TS1), while it reaches a peak value of about $\max\{|u_2(t)|\}|_\mathrm{HD} \approx 600\ \mathrm{mV}$ for the case of the loaded conductor loop (TS2). In the

HD-case, the electric field vector points in x-direction. Since the parallel pair of conductors point in y-direction, a maximum potential difference occurs with this field orientation. For the conductor pair with the open end, the conductor pair probes the potential generated by the electromagnetic field at a distance $d = 20\ \mu\mathrm{m}$. Hence, the shape interference voltage corresponds approximately to the shape of the applied field. The maximum amplitude can be roughly estimated by the potential difference $u_{\max} = \int_0^d E_0\,\mathrm{d}x = d \cdot E_0 = 20\ \mu\mathrm{m} \cdot 50\ \frac{\mathrm{kV}}{\mathrm{m}} = 1\ \mathrm{V}$. For both pulse shapes, the lowest interference (LD) is caused by a HPEM wave propagating in the x-direction with its electric field oriented in the direction of the y-axis (yellow lines). The maximum value of the interference voltages for both test structures is $\max\{|u_{1,2}(t)|\}|_{\mathrm{LD}} \approx 60\ \mathrm{mV}$ for the Gaussian excitation pulse and $\max\{|u_{1,2}(t)|\}|_{\mathrm{LD}} \approx 30\ \mathrm{mV}$ for the double-exponential excitation pulse. In the LD-case, the electric field vector points along the conductors, so that no high differential voltage is formed between the two conductors.

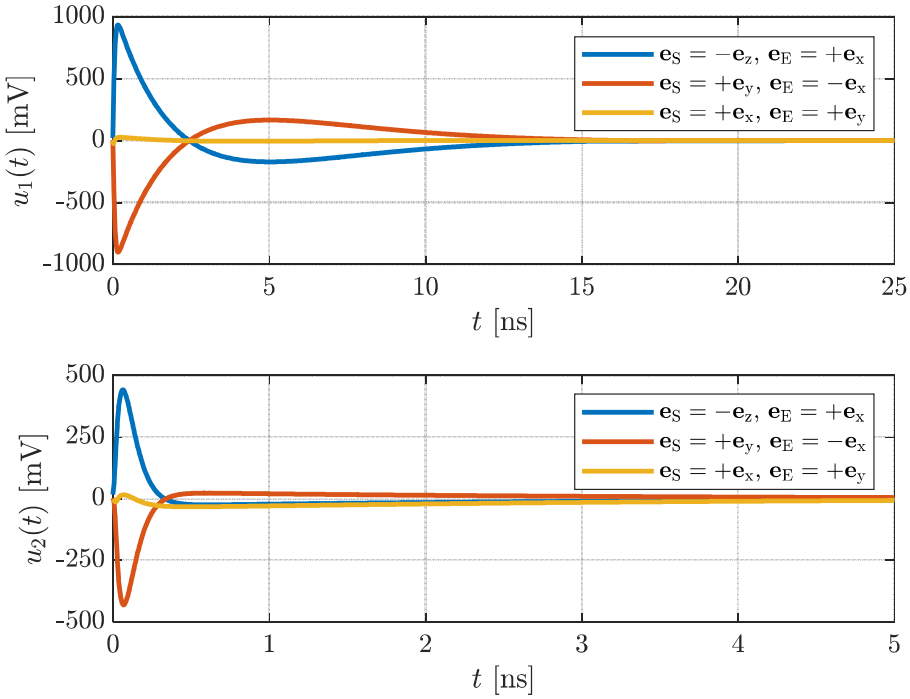

Figure 5: Interference voltages at the test structures without protection measures excited by a double-exponential pulse

3 Shielding by Using a Protective Grid

In this section, the protective effectiveness of a uniform protective grid is investigated.

3.1 Simulation Setup

The protective grid is built up by arranging metallic conductors (grey) crosswise above the test structures over the entire silicon substrate as shown in Figure 6 (not to scale). The metallic conductors are connected to the metallic surface below the silicon cuboid by vias (red) at the substrate edge. This results in a kind of Faraday cage that can shield the HPEM wave. The width of the conductors of the grid is $b = 10\ \mu\mathrm{m}$. The spacing of the grid is $a_{\mathrm{NPG}} = 10\ \mu\mathrm{m}$ for a narrow protective grid (NPG) and $a_{\mathrm{WPG}} = 40\ \mu\mathrm{m}$ for a wide protective grid (WPG). Neither the test structures nor the cross-section or the parameters of the IC model are changed compared to the previous section.

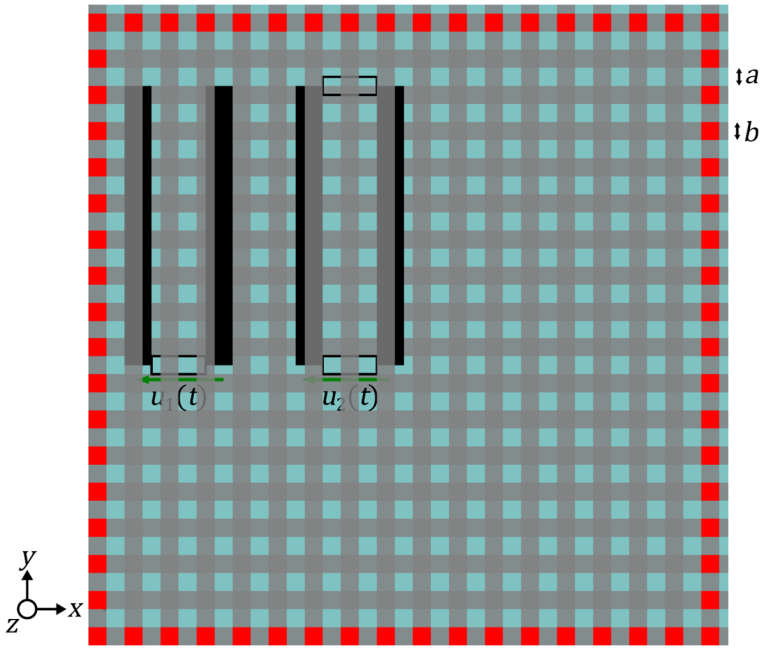

Figure 6: IC model with a protective grid, top view

For technical reasons, it may be necessary to connect the protective grid to the bottom side metal ground plane at only a few points. Therefore, in order to study the influence of reducing the number of contacts, the limiting case given by a protective grid connected to the metal surface only at a single point is investigated. For this purpose, only a single via is placed in the lower right corner in the simulation and further simulations are made.

3.2 Simulation Results

The same three combinations of direction of incidence and polarization of the HPEM wave are considered as in the previous section. Only the EM-simulation based results for the Gaussian excitation pulse are shown, since an excitation by a double-exponential pulse give similar results with respect to the peak magnitude of the interference voltages. Figure 7 shows the interference voltages at the test structures with protection using a narrow protective grid (grid spacing $10\ \mu\mathrm{m}$) excited by a Gaussian pulse. The combinations with the electric field vector orientated in x-direction (blue and red lines), which cause the highest interference for the unshielded case, show a reduction of the peak magnitude of the interference voltage to $\max\{|u_1(t)|\}|_{\mathrm{HD}}|_{\mathrm{NPG}} \approx 5\ \mathrm{mV}$ for the open pair of conductors and $\max\{|u_2(t)|\}|_{\mathrm{HD}}|_{\mathrm{NPG}} \approx 1\ \mathrm{mV}$ for the loaded pair of conductors. This corresponds to a reduction of the peak interference voltage by almost a factor of 200 $(46\ dB)$ for test structure 1 ($u_1(\mathrm{t})$) and even 600 $(55.6\ dB)$ for test structure 2 ($u_2(\mathrm{t})$). The combinations with the electric field vector orientated in y-direction (yellow lines), which cause the lowest interference for the unshielded case, show a reduction of the peak magnitude of the interference voltage to $\max\{|u_{1,2}(t)|\}|_{\mathrm{LD}}|_{\mathrm{NPG}} \approx 2\ \mathrm{mV}$ for the open as well as for the loaded pair of conductors. This corresponds to a reduction of the peak interference voltage by almost a factor of 30 $(29.6\ dB)$. The narrow protective grid reduces the interference voltage in the single-digit millivolt range in all cases.

Figure 8 shows the interference voltages at the test structures with protection using a wide protective grid (grid spacing $40\ \mu\mathrm{m}$) excited by a Gaussian pulse.

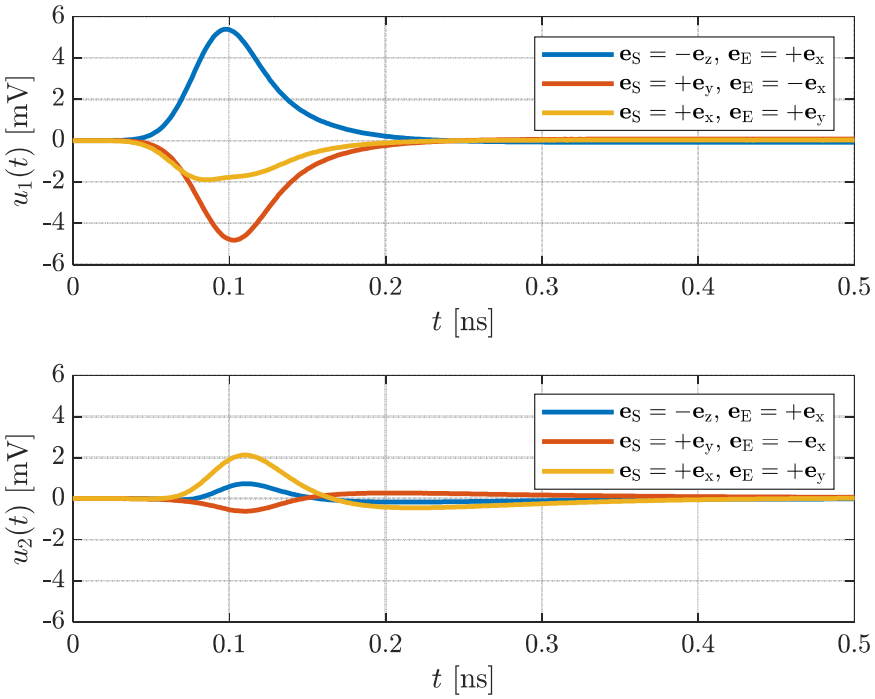

Figure 7: Interference voltages at the test structures protected by a narrow protective grid excited by a Gaussian pulse

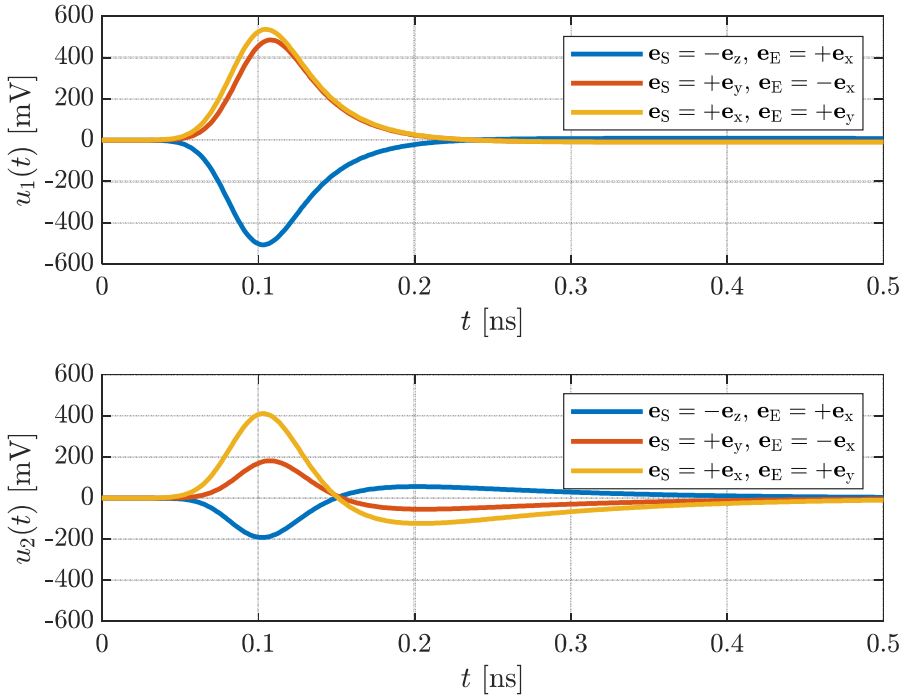

Figure 8: Interference voltages at the test structures protected by a wide protective grid excited by a Gaussian pulse

The combinations with the electric field vector orientated in x-direction show a peak magnitude of the interference voltage of $\max\{|u_1(t)|\}|_{\mathrm{HD}}|_{\mathrm{WPG}} \approx 500\ \mathrm{mV}$ for the open pair of conductors and $\max\{|u_2(t)|\}|_{\mathrm{HD}}|_{\mathrm{WPG}} \approx 200\ \mathrm{mV}$ for the loaded pair of conductors. This corresponds a reduction of the peak interference voltage by a factor of 2 ($6\ dB$) to 3 ($9.5\ dB$). In contrast, the combinations with the electric field vector orientated in y-direction show an increase in the peak magnitude of

the interference voltage to $\max\{|u_{1,2}(t)|\}|_{\mathrm{LD}}|_{\mathrm{WPG}} \approx 500\,\mathrm{mV}$ for the open and $\max\{|u_2(t)|\}|_{\mathrm{LD}}|_{\mathrm{WPG}} \approx 400\,\mathrm{mV}$ for the loaded pair of conductors. The reason for the decrease in shielding effectiveness may be that the wide protective grid acts as a kind of resonant structure for the HPEM pulse.
Figure 9 shows the interference voltages occurring at the test structures shielded by a narrow protective grid with a single contact to the ground plane (NPG,SC) when excited with a Gaussian pulse. The shielding effectiveness is reduced especially for the waves causing highest interference with a field vector orientated to the x-direction. The peak interference voltage at test structure 1 is $\max\{|u_1(t)|\}|_{\mathrm{HD}}|_{\mathrm{NPG,SC}} \approx 50\,\mathrm{mV}$ which is about ten times higher than compared to the narrow protective grid with many ground contacts, and the peak interference voltage at test structure 2 is $\max\{|u_2(t)|\}|_{\mathrm{HD}}|_{\mathrm{NPG,SC}} \approx 10\,\mathrm{mV}$ which is about five times higher. However, compared to the case without protection measures, where the voltage maxima were about $900\,\mathrm{mV}$ and $600\,\mathrm{mV}$, respectively, the shielding effect is still significant. The peak interference voltage for the incident wave in the x-direction is also increased compared to the narrow protective grid, but still within the small two digit mV range.

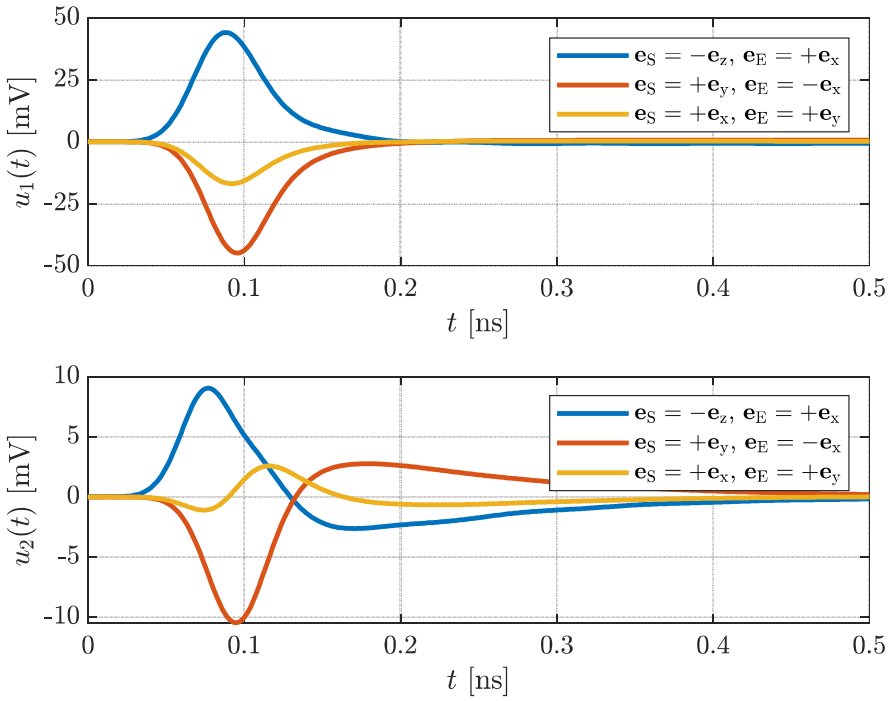

Figure 9: Interference voltages at the test structures protected by a narrow protective grid with a single contact to the ground plane excited by a Gaussian pulse

4 Conclusion

An EM simulation-based study of the effects of electromagnetic interference on integrated circuits has been presented. Scenarios without protective measures and with a protection by a metal grid are investigated. The results show that the interference voltages are significantly reduced by the protective grid. The choice of the grid spacing is crucial for the protection performance.

Literature

[1] M. Bäckström: The threat from intentional EMI against the civil technical infrastructure, 3rd European Survivability Workshop ESW 2006, 2006, pp. 16–19
[2] S. C. Tonder, S. Bieder, A. Czylwik, M. Willenbockel: Interference created by HPEM pulses at integrated circuit ports, Kleinheubacher Tagung, 23. – 25. Sept. 2019, Miltenberg, Germany
[3] IMST GmbH: EMPIRE XPU Software, Information available at: http://www.empire.de